Dendritic Cell-Derived Extracellular Vesicles Mediate Inflammation in Egg-Allergy Patients

Davis Tucis †, Georgina Hopkins †, Victoria James, David Onion, Lucy C. Fairclough *

Posted Date: 16 December 2025

doi: 10.20944/preprints202512.1321.v1

Keywords: type I hypersensitivity; allergy; dendritic cells; extracellular vesicles; T cells; Th2 cells

 doi:10.20944/preprints202512.1321.v1

Article

Dendritic Cell-Derived Extracellular Vesicles Mediate Inflammation in Egg-Allergy Patients

Davis Tucis [1,†], Georgina Hopkins [1,†], Victoria James [2], David Onion [1] and Lucy C. Fairclough [1,*]

[1] School of Life Sciences, The University of Nottingham, Nottingham NG7 2UH, UK

[2] School of Veterinary Medicine and Science, The University of Nottingham, Nottingham NG7 2UH, UK

* Correspondence: Professor Lucy Fairclough, lucy.fairclough@nottingham.ac.uk

[†] These authors contributed equally to the preparation of this manuscript.

Abstract

Atopic allergy is rising globally and placing a significant strain on healthcare systems, yet the understanding of the underpinning mechanisms of allergic sensitisation remains incomplete. Extracellular vesicles (EVs) have recently emerged as important mediators of immune modulation due to their diverse cargo and therefore may play a mechanistic role in allergic sensitisation development. Thus, this study investigated whether EVs released by activated dendritic cells (DCs) contribute to allergic sensitisation of the common egg allergen, ovalbumin (OVA). DCs were generated from human monocytes cultured with GM-CSF and IL-4, then stimulated with LPS and/or OVA. EVs were subsequently isolated using size-exclusion chromatography and added to freshly isolated naïve T cells at defined time points. T-cell responses were then analysed using spectral flow cytometry. The results highlight EVs derived from LPS or LPS+OVA-stimulated DCs enhanced IL-4 production and reduced IFN-γ production in naïve T cells from egg-allergic donors, indicating a shift toward a Th2 profile. In healthy donors, LPS-induced DC EVs also suppressed IFN-γ expression. Notably, EVs alone were insufficient to activate T cells without CD3/CD28 co-stimulation, suggesting that EVs may function as a "third signal" shaping T-cell polarisation. These findings highlight a potential role for DC-derived EVs in initiating allergic sensitisation.

Keywords: type I hypersensitivity; allergy; dendritic cells; extracellular vesicles; T cells; Th2 cells

1. Introduction

Allergic diseases driven by IgE-mediated type-I hypersensitivity have become a major global health challenge, with food allergy prevalence reaching 8–10% in children and 3–6% in adults in Westernized countries [1,2]. For egg allergy, it most commonly presents in infancy with a prevalence of about 2% in children and 0.1% in adults [3].

Allergic sensitisation is the first stage in developing an allergy. The critical step in allergic sensitisation is the aberrant activation of naïve $CD4^+$ T cells by professional antigen-presenting cells, particularly dendritic cells (DCs), resulting in Th2 polarisation characterised by IL-4, IL-5, and IL-13 secretion, IgE class-switching, and subsequent binding to mast cells and basophils [4,5]. Naïve T-cell priming classically requires three signals: T-cell receptor recognition of peptide–MHC-II complexes (signal 1), co-stimulation (primarily CD80/CD86–CD28) (signal 2), and polarising cytokines that dictate lineage commitment (signal 3) [6].

However, intercellular communication in immunity extends well beyond direct cell–cell contact and cytokines. Extracellular vesicles (EVs), a heterogeneous family of lipid-enclosed particles ranging from 30 to 1000 nm, are now established as important carriers of bioactive cargo including proteins, lipids, mRNAs, miRNAs, and intact MHC–peptide complexes [7–9]. Dendritic cells constitutively release EVs, and their biogenesis, cargo loading, and surface composition are profoundly modulated by maturation status and environmental stimuli such as pathogen-associated molecular patterns (e.g.,

 doi:10.20944/preprints202512.1321.v1

lipopolysaccharide, LPS) or allergens [10–12]. Numerous murine and human studies have demonstrated that DC-derived EVs can transfer allergen or MHC–allergen complexes to T cells and promote Th2-skewed responses. For instance, EVs from DCs can carry major cat allergen Fel d 1 and induce allergic immune response[13]. These findings have led to the hypothesis that EVs may function as an autonomous "signal 3" or amplify classical priming pathways during allergic sensitisation [{Gutiérrez-Vázquez, 2013 #360] [14]].

Despite substantial progress, several methodological limitations have prevented definitive conclusions regarding the specific contribution of human DC-derived EVs to allergy. Most functional studies have relied on differential ultracentrifugation, which co-isolates soluble proteins, immune complexes, and lipoproteins that independently affect T-cell responses [15,16]. Residual cytokines frequently co-purified with EVs can mask vesicle-specific effects. Many assays have employed total or memory $CD4^+$ T cells rather than rigorously purified naïve populations, making it difficult to distinguish genuine sensitisation from recall responses. Furthermore, prolonged DC culture in serum-containing media introduces substantial bovine EV contamination, breaking current MISEV guidelines [7,17]. Finally, direct comparative studies between healthy individuals and patients with confirmed allergy using cytokine-depleted, highly purified EVs remain scarce.

To address these challenges, the present study established a fully human, MISEV-compliant *in vitro* platform that incorporates optimized monocyte-derived DC differentiation with short-term (24 h) maturation in serum-free medium, EV isolation by size-exclusion chromatography with validated depletion of soluble cytokines, comprehensive multimodal EV characterization, and repeated exposure of stringently isolated naïve $CD4^+$ T cells from healthy donors and individuals with egg allergy, both with and without CD3/CD28 co-stimulation. This work aimed to determine whether highly purified human DC-derived EVs generated under resting, inflammatory (LPS), allergen (OVA), or combined conditions can activate and polarise naïve $CD4^+$ T cells, and whether their immunomodulatory effects differ between healthy and allergic individuals, thereby clarifying the role of EVs in the early events of human allergic sensitisation.

2. Results

2.1. Generation of Dendritic Cells in Serum-Free Conditions for EV Analysis

To ensure purity in EV isolates for assessing allergic sensitisation, strategies were implemented to deplete platelet-derived EVs and soluble cytokines, which could confound T cell responses. Platelet contamination in serum-supplemented media was examined following CD14+ monocyte isolation (Figure 1Ai). Forward scatter analysis of CD41/CD61 events revealed a marked reduction in platelet counts post-isolation of CD14+ magnetic isolation (Figure 1Aii-iii). Due to the requirement of culturing monocytes in media containing serum to maintain viability, EV carryover from the monocyte-to-DC culture was mitigated by swapping RPMI + 10% FBS to serum-free X-VIVO prior to stimulation (Figure 1B). ImageStreamX analysis showed a ~70% decrease in baseline EV concentration post-swap. Furthermore, when compared to LPS-stimulated DC production of EVs, media EV presence accounted for less than 1% of total EVs produces by DCs.

Monocyte-derived DCs were then stimulated with 100 ng/mL LPS, 10 µg/mL OVA, or OVA+LPS for 24 or 48 h to assess both viability (Figures 1Ci-ii) and maturation marker expression (Figure 1D) of the DCs. Viability, assessed by Zombie Aqua staining, exceeded 70% at 24 h across conditions, meeting MISEV guidelines, but declined slightly at 48 h. Maturation was also evaluated via flow cytometry for costimulatory (CD80, CD83, CD40) and adhesion/activation (CD209, HLA-DR, CD14) markers. At 24 h, LPS and OVA+LPS stimulation upregulated CD80, CD83, and CD40 relative to immature/unstimulated DCs, indicative of full maturation (Figure 1D). OVA alone elicited minimal changes. At 48 h, expression waned, mirroring viability trends. CD209 decreased selectively in LPS-stimulated DCs, while HLA-DR increased. CD14 remained low across conditions (Figure 1D). These data confirm that 24 h stimulation with LPS or OVA+LPS in X-VIVO yields viable, mature DCs with

 doi:10.20944/preprints202512.1321.v1

minimal contaminants from serum-based and platelet-derived EVs, optimizing EV production for T cell studies.

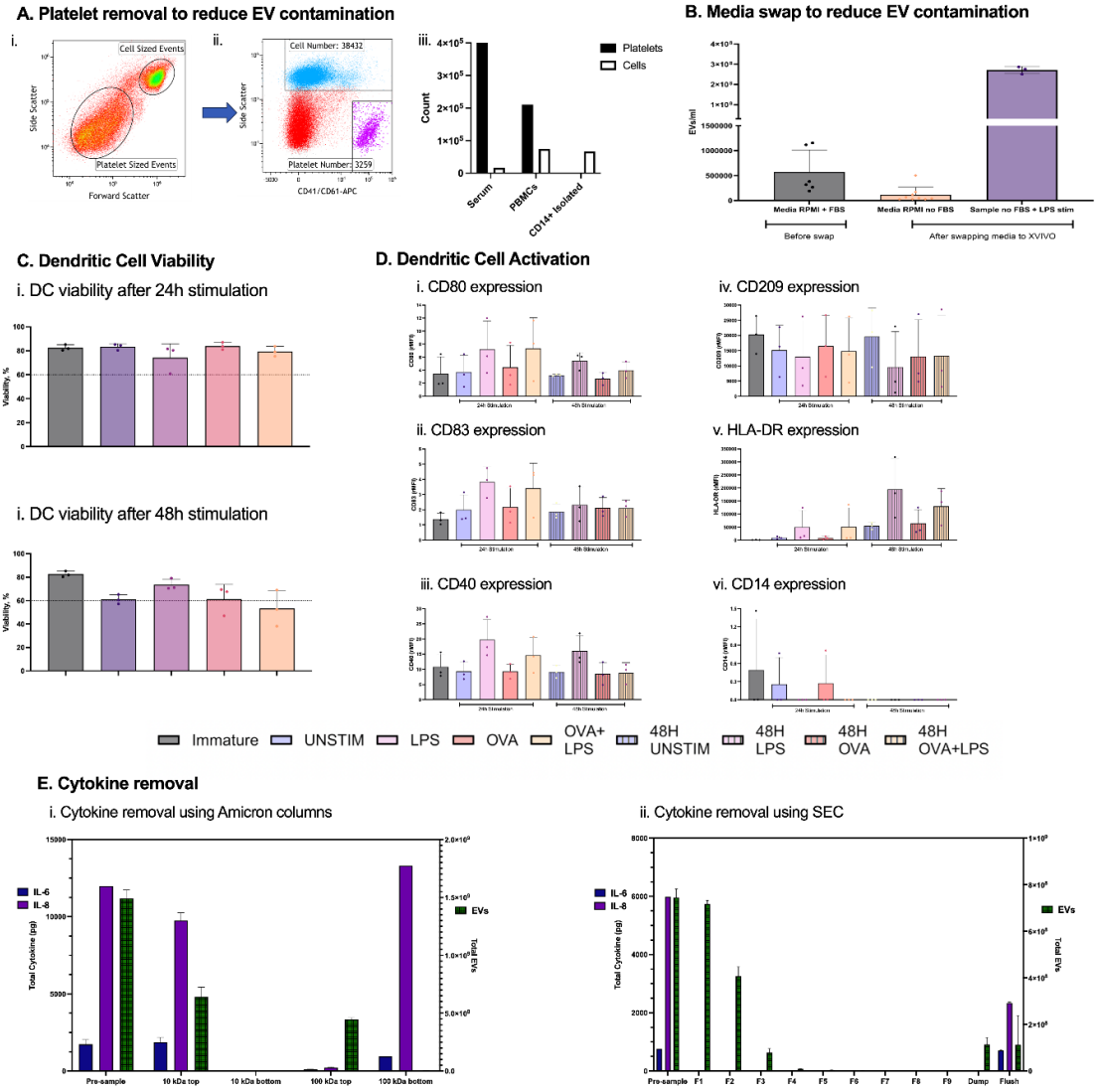

Figure 1. DC-EV Optimization. Reduction of contaminating EVs from platelets by CD14+ magnetic isolation (Ai, ii, iii) and media FBS after complete media swap from RPMI + 10% FBS to serum-free X-VIVO 15 on day 5, immediately before DC stimulation (B). Viability assessed by Zombie Aqua and Maturation marker expression (rMFI) on DCs after 24 h and 48 h stimulation (C-D). Comparison of cytokine versus EV separation efficiency using Amicon ultrafiltration (10 kDa and 100 kDa) (Ei) and automated size-exclusion chromatography (qEV/35 nm columns) (Eii). Primary human DC cell supernatants were spiked with recombinant IL-6 and IL-8, processed, and analysed by ELISA (cytokines) and calcein-AM/ImageStreamX (EVs). n = 3 independent donors.

Concerning cytokine removal, molecular weight filters are often used for concentrating EVs after isolation, but their ability to remove cytokines from a sample is yet to be tested. EVs are often concentrated from larger pools of media before SEC. We tested for the presence of cytokines and total EVs pre and post concentration with molecular weight cut off filters and size exclusion chromatography. IL-6 and IL- 8 were present pre- and post-concentration, highlighting they should not be used to be deplete these cytokines. While more concentrated the total EV numbers were also reduced by molecular weight cut off filtration demonstrating concentration with these methods should only be used if experimentally necessary. SEC depleted IL-6 and IL-8 below detectable thresholds in all EV rich fractions and was used without pre-concentration for further experiments. (Figure 1E).

 doi:10.20944/preprints202512.1321.v1

Activated and mature human monocyte-derived DCs produce copious amounts of IL-6 and IL-8, thus, the presence of these cytokines was measured in the EV fractions after SEC, and after Amicon filter column centrifugation.

The results show both IL-6 and IL-8 were still present in the top chamber of filters where EVs were also present, in both 10 kDa and 100 kDa filters (Figure 1Ei), suggesting these are not suitable for EV/cytokine separation. Furthermore, analysis of EVs showed that both 10 and 100 kDa columns lose EVs after centrifugation. In contrast, there were no cytokines detected in SEC fractions 1 to 9 (Figure 1Eii), while maintaining the majority of EVs, with most EVs present in fractions 1-5. For future experiment, samples generated where isolated by SEC and fractions 1-x combined to ensure EVs could be added to naive T cells without any contaminating cytokine.

2.2. Characterisation of EVs Generated by DCs

EV preparations from monocyte-derived DCs were characterised using multimodal imaging and flow-based analysis to confirm morphology, size, and molecular markers. Transmission electron microscopy (TEM) revealed characteristic cup-shaped, collapsed vesicles with diameters of 50-150 nm (Figure 2Ai). Confocal microscopy of calcein-AM (green)- and lipid dye DiD (red)-stained EVs displayed punctate, colocalized signals consistent with intact lipid bilayers (Figure 2Aii). Super-resolution nanoscopy (ONI) identified tetraspanin distribution, with CD81, CD63, and CD9 exhibiting clustered expression on vesicle surfaces (Figure 2Aiii). For high-throughput analysis, EVs were also evaluated on Imaging flow cytometry using 130 nm calibration nanobeads to establish size thresholds (Figure 2Bi). Events below this threshold were gated as EVs (Figure 2Bii), with further refinement to exclude particles >1 μm via brightfield area (Figure 2Biii). Single calcein-AM-positive vesicles were isolated using spot count masking (Figure 2Biv), and including only calcein-positive events (Figure 2Bv), yielding a focused EV population with modal intensity ~60 (Figure 2Bvi). Tetraspanin expression was then profiled on calcein-gated EVs from healthy and egg-allergic donor DCs using a REAfinity antibody panel (Figure 2C). EVs predominantly expressed CD9 and CD81 in both donor types, with lower CD63 levels. Co-expression analysis revealed frequent single (CD9/CD81) and double (CD9/CD81) positivity, alongside triple-positive subpopulations. These characterisations validate the purity and identity of DC-derived EVs for downstream functional assays.

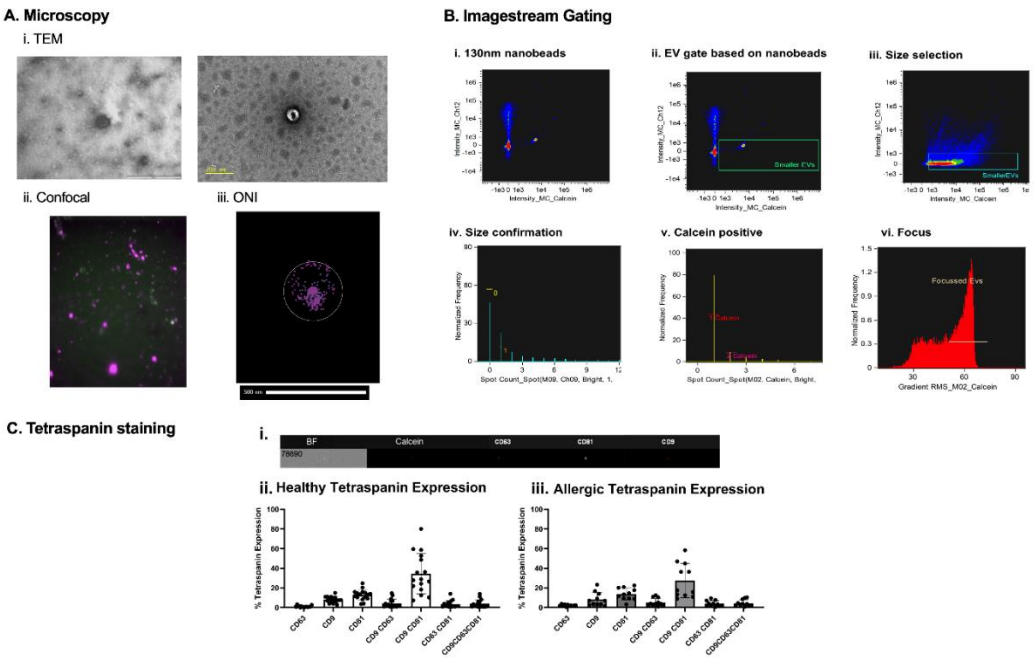

Figure 2. EV analysis. Extracellular vesicles under different microscopes. EVs were observed under TEM (Ai). Utilizing confocal microscopes features, calcein-AM stained and lipid dye DID stained EVs were overlayed together (Aii). Super-resolution microscope (ONI) allowed the staining of tetraspanins CD81, CD63 and CD9, to

 doi:10.20944/preprints202512.1321.v1

observe the number of copies on each EV in the sample (Aiii). Nanobeads of known refractive index and sized at 130nm were run on ISX to determine their positioning on the machine (Bi.). Based on the interest of only in small EVs, everything below 130nm beads was selected (Bii.). The sizing gate was then applied to EV samples (Biii). Knowing that ISX brightfields minimum pixel range is 0.9 µm, it was possible to create a gate ensuring objects larger than 0.9 µm would be excluded (Biv.). To ensure objects selected were intact EVs, a calcein+ gate was introduced (v.). To reduce artifacts and increase accuracy of tetraspanin expression on EVs, only in-focus EVs were selected (Bvi). (Ci) ImageStream X MkII imaging of a single EV showing the EV brightfield image (BF), and calcein, CD63 PE, CD81 PE-Vio 615, and CD9 APC fluorescence. (Cii) % of tetraspanin expression on DC-derived EVs from healthy and allergic individuals (Ciii).

2.3. Minimal Impact of DC-Derived EVs on Naive T Cell Viability, Activation and Cytokine Production

Naive T cells from healthy donors and allergic individuals were exposed three times to EVs derived from unstimulated, LPS-stimulated, OVA-stimulated, or OVA+LPS-stimulated DCs. Viability of T cell remained high across all conditions and donor types (Figure 3A).Activation of T cells, as identified by early activation marker CD69 expression, was negligible in both groups (Figure 3B), indicating limited T cell priming by EVs alone. Furthermore, intracellular cytokine staining revealed minimal Th1/Th2/Th17-associated responses following EV exposure (namely IFN-γ [Figure 3C], IL-4 [Figure 3D], TNF-α [Figure 3E] and IL-2 [Figure 3F]). These data demonstrate that DC-derived EVs alone elicit no stimulation of naive T cells, regardless of DC stimulation state or donor allergy status.

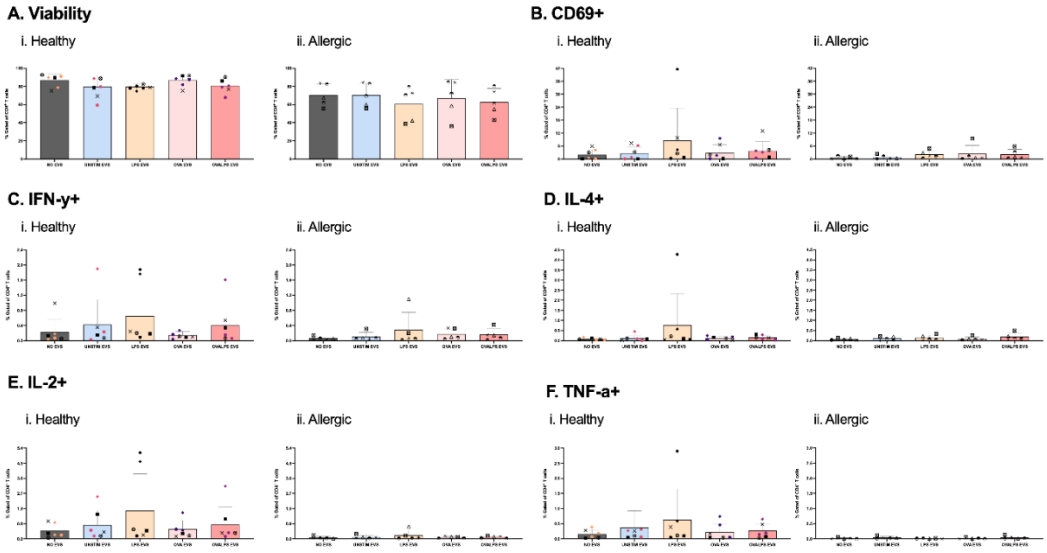

Figure 3. Effect of EVs alone on T cell viability and function. Naive T cells were plated in 96-well plate. Each well afterwards was stimulated with dendritic cell-derived EVs added in 3 doses. DCs were stimulated with 100ng/ml of LPS, 10µg/ml of OVA, 50ng/ml of LPS and 10µg/ml of OVA, and unstimulated, PBS was added as control. T cells were stimulated every 24h for 3 times, only 3rd dose results shown. Cytokine expression was measured after 42h, following 30h stimulation of EVs and 12h incubation with PTI, CD69 (B), IFN-y (C), IL-4 (D), TNF-a), IL-2 (F). Study included 7 healthy and 5 allergic participants. Statistical analysis was performed in GraphPad Prism using one-way ANOVA, $p<0.05$.

2.4. Enhanced T Cell Activation and Th2 Skewing with CD3/CD28 Co-Stimulation

To evaluate the synergistic effects of DC-derived EVs with concomitant T cell receptor signalling, naive T cells from healthy and allergic donors also underwent three sequential exposures to EVs (generated from unstimulated, LPS-stimulated, OVA-stimulated, or OVA+LPS-stimulated DCs) in the presence of anti-CD3/CD28 co-stimulation. This co-stimulation amplified overall T cell responses compared to EV exposure alone. Specifically, T cell viability was largely preserved across conditions (Figure 4A), exceeding 80% in healthy donors and ~70% in allergic donors. CD69 was expressed in

 doi:10.20944/preprints202512.1321.v1

both donor types after 96-hour culture (Figure 4B), however, T cells from allergic patients displayed significantly lowered activation in the absence of EVs or when EVs were derived from unstimulated DCs, when compared to EVs derived from either LPS or LPS/OVA-stimulated DCs (Figure 4Bii).Overall, the percentage of IFN-γ-producing T cells (Th1 marker) was higher in T cells from healthy donors (20-30% positive; Figure 4Ci) but comparatively subdued in T cells from allergic donors (10-20%; Figure 4Cii), but this was irrespective of the presence or absence of EVs. Conversely, the percentage of IL-4-producing T cells (Th2 marker) in healthy samples was found in modest levels (Figure 4Di), as were allergic T cells (Figure 4Dii), however, in allergic individuals, the addition of EVs generated from either LPS or LPS+OVA stimulated DCs significantly increased the percentage of IL-4 positive T cells. The percentage of IL-2 positive T cells, supporting T cell expansion, was comparable in both groups (Figure 4E), as were the percentage of TNF-α positive T cells (pro-inflammatory marker), and again this was irrespective of the presence or absence of EVs. These results illustrate that CD3/CD28 co-stimulation unmasks EV-driven T cell activation, with allergic donors showing biased Th2 responses that could drive allergic disease progression.

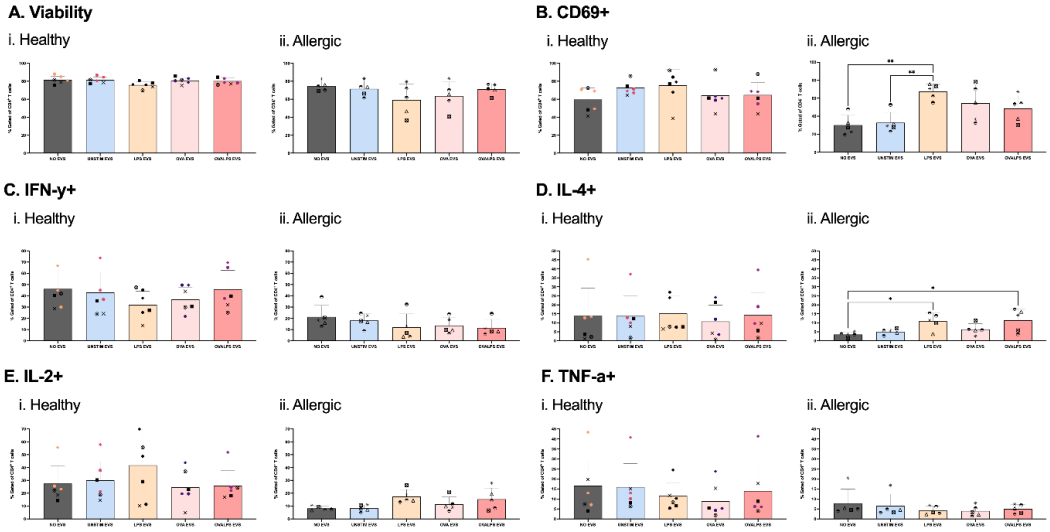

Figure 4. EVs as Signal 3 in T cell activation. Naive T cells were plated in 96-well plate with co-stimulation of coated 2µg/ml CD3 and direct 2µg/ml CD28. Each well afterwards was stimulated with dendritic cell-derived EVs added in 3 doses. DCs were stimulated with 100ng/ml of LPS, 10µg/ml of OVA, 50ng/ml of LPS and 10µg/ml of OVA, and unstimulated, PBS was added as control. T cells were stimulated every 24h for 3 times (i., ii., iii.,). Cytokine expression was measured after 42h, following 30h stimulation of EVs and 12h incubation with PTI, CD69 (B), IFN-y (C), IL-4 (D), TNF-a), IL-2 (F) Study included 7 healthy and 5 allergic participants. Statistical analysis was performed in GraphPad Prism using one-way ANOVA, $p<0.05$.

2.5. Unsupervised Clustering Analysis Reveals Differences in Baseline T Cell Responses Generated in Healthy and Allergic Individuals

To further delineate the effects of EVs generated from PBS-stimulated DCs (i.e. baseline effects), on naive T cell subsets between healthy and allergic donors, flow cytometry data from viable CD3+CD4+ T cells from four healthy and four allergic donors were subsampled (5000 events/donor) and subjected to FlowSOM clustering (20 meta-clusters) incorporating surface (CD45RA, CD8, CD56, CD27, CD28, CCR7, CD69) and intracellular (IL-2, IL-4, IFN-γ, TNF-α) markers. Figure 5A presents the tSNE visualisation of FlowSOM clusters, Figure 5B is the tSNE visualisation of marker density, and Figure 5C presents the percentage of Tells found in each identified FlowSOM cluster, with cluster 20 comprising the largest proportion of events. Of the 25 clusters identified, population distributions differed significantly across 20 clusters (Figure 5D; *$p < 0.05$, Mann-Whitney U). Healthy donor T cells enriched clusters 1-5, 9-11, and 17 (Figure 5Ei), were characterised by high CD45RA, CD27, CD28, and CCR7 (naive/memory precursor phenotype) alongside modest IL-2/TNF-α. Conversely, allergic

 doi:10.20944/preprints202512.1321.v1

T cells dominated clusters 6, 16, 18, 20, and 24 (Figure 5Eii), were marked by elevated IL-4, IFN-γ, and TNF-α with reduced CD45RA/CD27.

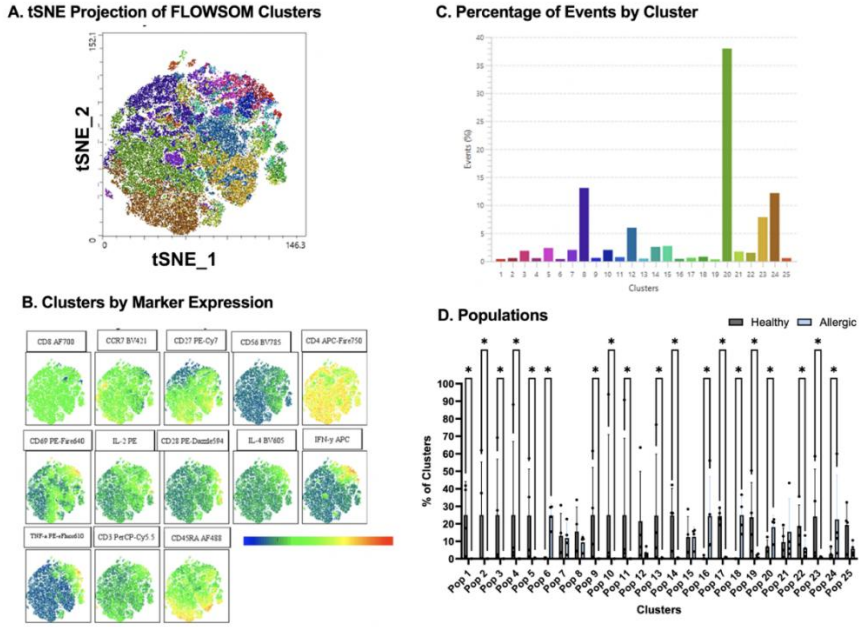

E. Significant population marker expression

i. Healthy

Populations	CD45-RA	CD3	CD8	CD4	CD56	CD27	CD28	CCR7	CD69	IL-2	IL-4	IFN-γ	TNF-α
Pop 1	Dim/mod	Bri	Neg	Bri	Neg	Mod	Bri	Neg	Bri	Bri	Bri	Bri	Bri
Pop 2	Mod	Bri	Neg	Bri	Neg	Mod	Mod	Neg	Bri	Mod	Bri	Bri	Bri
Pop 3	Dim	Bri	Neg	Bri	Neg	Mod	Mod	Dim	Bri	Dim/mod	Mod	Bri	Bri
Pop 4	Neg/dim	Bri	Neg	Bri	Neg	Mod	Mod	Dim	Mod	Mod	Mod	Bri	Mod
Pop 5	Dim	Bri	Neg	Bri	Neg	Dim	Dim	Mod	Mod	Dim	Dim	Mod/bri	Mod
Pop 9	Mod	Bri	Neg	Bri	Neg	Mod	Bri	Dim/mod	Bri	Bri	Bri	Bri	Bri
Pop 10	Bri	Bri	Neg	Bri	Neg	Bri	Dim/mod	Dim/mod	Bri	Dim/mod	Mod	Bri	Mod
Pop 11	Mod	Bri	Neg	Bri	Neg	Mod	Dim/mod	Mod	Mod	Mod/bri	Dim/mod	Bri	Dim/mod
Pop 13	Neg/dim	Bri	Neg	Bri	Neg	Dim	Bri	Dim/mod	Mod	Mod/bri	Dim	Mod/bri	Bri
Pop 14	Mod	Bri	Neg	Bri	Neg	Bri	Dim	Mod	Mod	Mod	Dim	Mod	Dim
Pop 17	Mod	Bri	Neg	Bri	Neg	Bri	Bri	Mod	Mod	Mod/bri	Mod	Dim	Bri
Pop 19	Neg/dim	Bri	Neg	Bri	Neg	Neg	Mod	Mod	Bri	Dim	Dim/mod	Neg	Mod
Pop 22	Mod	Bri	Neg	Bri	Neg	Dim	Dim	Mod	Mod/bri	Mod	Dim	Neg	Dim
Pop 23	Bri	Bri	Neg	Bri	Neg	Bri	Dim	Dim	Mod	Dim/mod	Neg	Neg	Neg

ii. Allergic

Populations	CD45-RA	CD3	CD8	CD4	CD56	CD27	CD28	CCR7	CD69	IL-2	IL-4	IFN-γ	TNF-α
Pop 6	Dim	Bri	Neg	Bri	Neg	Neg/dim	Neg/dim	Mod/bri	Mod	Neg	Neg/dim	Dim	Neg/dim
Pop 16	Mod	Bri	Neg	Bri	Neg	Bri	Bri	Bri	Mod	Bri	Neg/dim	Dim	Mod/bri
Pop 18	Bri	Bri	Neg	Bri	Neg	Mod/bri	Bri	Bri	Dim	Neg/dim	Neg/dim	Dim	Bri
Pop 20	Mod	Bri	Neg	Bri	Neg	Mod	Neg/dim	Bri	Neg/dim	Neg/dim	Neg	Neg	Neg
Pop 24	Bri	Bri	Neg	Bri	Neg	Bri	Dim	Dim	Mod	Dim/mod	Neg/dim	Neg	Neg

Figure 5. Comparison between healthy and allergic using unbiased clustering analysis following culture with PBS-stimulated DC-derived EVs. Following cluster explorer plugin, a multi-coloured tNSNE plot was made (A) and individual marker clusters were produced from tSNE plot (B). Clusters were separated based on their % (C). Populations between healthy and allergic groups were analysed for significant differences using Mann-Whitney Tests $p<0.05$ (D). Significant populations were split between healthy and allergic groups, and their marker expression was colour coded - Negative (red), Negative/dim (orange), DIM (pale yellow), Dim/moderate (pale green), Moderate (light green), Moderate/bright (green), Bright (dark green) (Ei.,ii). N= 4 healthy donors, 4 allergic donors.

2.6. Unsupervised Clustering Analysis of T Cells Exposed to EVs Derived from LPS-Stimulated DCs Reveals Differences in T Cell Responses Generated in Healthy and Allergic Individuals

Having identified differences in both the percentage of CD69-expressing T cells and the percentage of IL-4-producing T cells in the allergic group following addition of EVs generated from DCs stimulated with LPS, viable CD3+CD4+ naive T cells from four healthy and four allergic donors, stimulated with anti-CD3/CD28 plus EVs from LPS-stimulated DCs, were subsampled (5000 events/donor) and clustered via FlowSOM . 20 meta-clusters were identified using surface (CD45RA, CD8, CD56, CD27, CD28, CCR7, CD69) and intracellular (IL-2, IL-4, IFN-γ, TNF-α) markers. Figure

 doi:10.20944/preprints202512.1321.v1

6A presents the tSNE visualisation of FlowSOM clusters, Figure 6B is the tSNE visualisation of marker density, and Figure 6C presents the percentage of Tells found in each identified FlowSOM cluster, with cluster 1 dominating. Thirteen clusters exhibited significant population disparities (*$p < 0.05$, Mann-Whitney U; Figure 6D). Healthy T cells preferentially populated clusters 3, 4, 6, 7, 11, 14, and 18 (Figure 6Ei), defined by high CD45RA, CD27, CCR7, and IL-2/TNF-α (naive/effector precursor traits). Allergic T cells enriched clusters 1, 5, 9, and 16 (Figure 6Eii), particularly the dominant cluster 1 (CD45RA+, CD3+, CD4+, CD27+, CCR7+, CD69 low/-), marked by minimal activation and subdued cytokine expression (IL-2/IL-4/IFN-γ/TNF-α low). This LPS-EV exposure preserved donor-specific divergences, with allergic enrichment in minimally activated subsets implying selective Th2 priming or anergy induction by inflammatory EVs in sensitised individuals.

No clustering differences were observed following repeated exposure to EVs from unstimulated, OVA-stimulated, or OVA+LPS-stimulated DCs (see supplementary figures x).

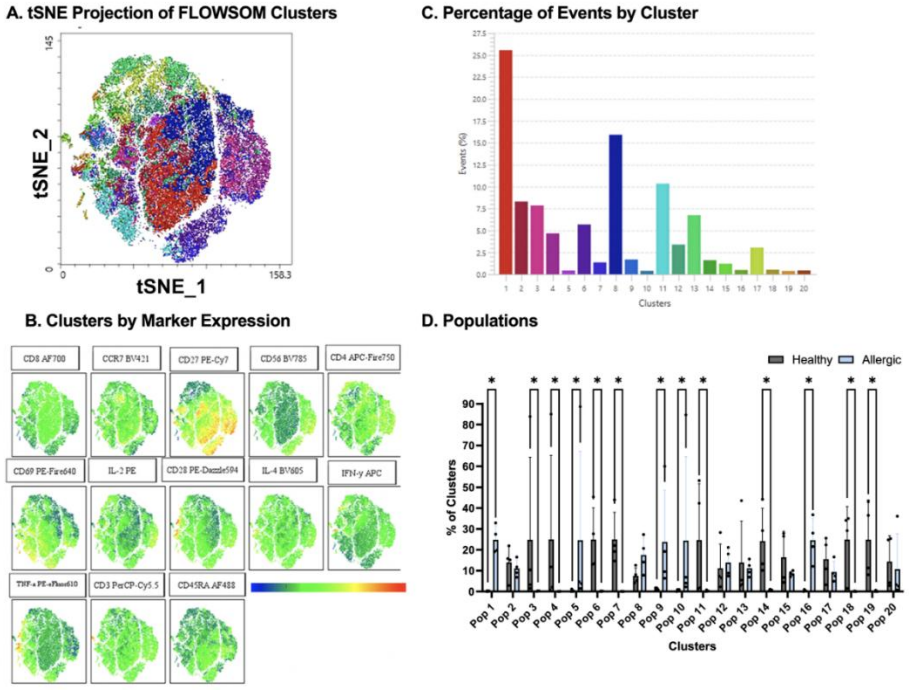

E. Significant population marker expression

i. Healthy

Populations	CD45-RA	CD3	CD8	CD4	CD56	CD27	CD28	CCR7	CD69	IL-2	IL-4	IFN-y	TNF-a
Pop 3	Dim	Bri	Neg	Mod	Neg	Mod	Dim	Bri	Mod	Mod	Mod	Dim	Dim
Pop 4	Dim	Bri	Neg	Bri	Neg	Bri	Neg/dim	Dim	Neg/dim	Neg/dim	Dim	Dim	Neg/dim
Pop 6	Mod	Bri	Neg	Bri	Neg	Bri	Bri	Bri	Mod	Bri	Dim/Mod	Mod	Bri
Pop 7	Bri	Bri	Neg	Bri	Neg	Bri	Mod	Bri	Bri	Dim	Dim/Mod	Neg/dim	Neg/dim
Pop 11	Bri	Bri	Neg	Mod	Neg	Neg	Neg/dim	Neg/dim	Mod	Mod	Neg/dim	Dim	Dim
Pop 14	Neg/dim	Bri	Neg	Bri	Dim	Mod	Bri	Mod	Bri	Bri	Bri	Bri	Bri
Pop 18	Mod	Bri	Neg	Bri	Dim	Bri	Mod	Mod	Mod	Bri	Mod/Bri	Mod	Dim
Pop 19	Bri	Bri	Neg	Bri	Dim	Bri	Mod	Dim	Bri	Mod	Mod	Neg/dim	Bri

ii. Allergic

Populations	CD45-RA	CD3	CD8	CD4	CD56	CD27	CD28	CCR7	CD69	IL-2	IL-4	IFN-y	TNF-a
Pop 1	Mod	Bri	Neg	Bri	Neg	Bri	Neg/dim	Bri	Mod	Dim	Dim/Mod	Neg/dim	Neg/dim
Pop 5	Dim	Bri	Neg	Bri	Neg	Bri	Neg/dim	Neg/dim	Neg/dim	Neg/dim	Dim	Mod	Neg/dim
Pop 9	Dim	Bri	Neg	Bri	Neg	Bri	Mod	Dim	Bri	Dim	Dim/Mod	Bri	Neg/dim
Pop 10	Neg/dim	Bri	Neg	Bri	Dim	Bri	Mod	Bri	Bri	Mod	Mod	Neg/dim	Mod
Pop 16	Neg/dim	Bri	Neg	Bri	Dim	Bri	Dim	Dim	Neg/dim	Mod	Neg/dim	Dim	Neg/dim

Figure 6. Comparison between healthy and allergic using unbiased clustering analysis following culture with LPS-stimulated DC-derived EVs. Following cluster explorer plugin, a multi-coloured tNSNE plot was made (A) and individual marker clusters were produced from tSNE plot (B). Clusters were separated based on their % (C). (C). Populations between healthy and allergic groups were analysed for significant differences using Mann-Whitney Tests $p<0.05$ (D). Significant populations were split between healthy and allergic groups, and their marker expression was colour coded - Negative (red), Negative/dim (orange), Dim (pale yellow), Dim/moderate (pale green), Moderate (light green), Moderate/bright (green), Bright (dark green) (Ei.,ii). N= 4 healthy donors, 4 allergic donors.

 doi:10.20944/preprints202512.1321.v1

3. Discussion

The present study establishes a rigorous, MISEV-compliant human *in vitro* platform to evaluate the immunomodulatory effects of dendritic cell-derived extracellular vesicles (DC-EVs) on naïve $CD4^+$ T cells polarisation in the context of egg allergy. Our findings indicate that DC-EVs isolated by size-exclusion chromatography (SEC) with cytokine depletion showed minimal impact on T-cell viability, CD69 expression, or cytokine secretion in the absence of TCR signalling (both signal 1 and 2). This observation underscores the limitations of earlier studies using ultracentrifugation, which often co-isolates soluble factors capable of independently driving T-cell responses [18,19].In addition, use of SEC-purified EVs aligns with recent reports emphasizing the need for contaminant-free preparations to accurately evaluate vesicle-specific functions [20].

However, when the EVs are combined with signal 1 and 2 co-stimulation (i.e. CD3/CD28), EVs from LPS and OVA+LPS-stimulated DCs promote activation and a shift toward Th2 cytokine production, particularly IL-4, which is more pronounced in allergic donors. This allergen-specific Th2 bias was accompanied by reduced IFN-γ, suggesting a role for DC-EVs in amplifying Th2 polarization during sensitization.

These results significantly add to prior work on DC-EVs in allergy. For instance, Fang et al. showed that plasma EVs from allergic rhinitis patients exhibit antigen-presenting properties and drive Th2 differentiation [21], while Molfetta et al. demonstrated that mast cell-derived EVs amplify allergic inflammation via immune complex transfer [22]. In murine models, OVA-loaded mesenchymal stem cell-EVs in contrast have shown immunosuppression and prevention of allergic sensitization and inflammation [23,24].

High-dimensional FlowSOM analysis further highlighted baseline differences in naïve T-cell subsets between healthy and allergic donors, with T cells from allergic donors showing subtle enrichment in low-activation clusters. OVA-EV exposure eliminated these differences, while LPS-EVs preserved donor-specific patterns. The enhanced IL-4 response to OVA-EVs in allergic donors suggests that DC-EVs may sustain Th2 memory in established allergy, contributing to persistence beyond infancy. This aligns with evidence that allergen-bearing EVs can facilitate remote antigen presentation, offering opportunities for EV-based diagnostics or therapies, such as targeted depletion during desensitization [25,26].

In summary, our data demonstrate that purified DC-EVs serve as effective signal 3 modulators in naïve T-cell priming, with OVA+LPS-matured EVs preferentially inducing IL-4 in the context of egg allergy. These findings also highlight the need for standardized EV isolation and provide a foundation for exploring EVs as biomarkers or intervention targets in allergic sensitization. Future studies should incorporate longitudinal donor sampling and multi-omics of EV cargo to further delineate mechanisms.

4. Materials and Methods

4.1. PBMC Isolation

Whole blood (50 mL) was collected from healthy and egg-allergic human volunteers into EDTA-coated tubes (approved by the NHS Health Research Authority Research Ethics Committee (Ref 21/SC/0183)). Egg-allergic patients were identified using NHS records of GP notes stating adverse reactions to egg and/or positive allergy testing results. The blood was diluted 1:1 (v/v) with phosphate-buffered saline (PBS) supplemented with 2% fetal bovine serum (FBS) (Merck, UK). SepMate™ tubes (StemCell Technologies, UK) were pre-filled with 15 mL Histopaque-1077 (Merck, UK), and the diluted blood was carefully layered atop the density gradient. Tubes were centrifuged at 1200 × g for 10 min at room temperature with the brake engaged. The peripheral blood mononuclear cell (PBMC)-containing buffy coat layer was aspirated and transferred to a new 50 mL conical tube, then diluted to 50 mL with PBS + 2% FBS. Cells were pelleted by centrifugation at 400 × g for 8 min at room temperature, and the supernatant was discarded. This washing step was repeated

 doi:10.20944/preprints202512.1321.v1

once more to remove residual Histopaque and cellular debris. Isolated PBMCs were resuspended in complete RPMI 1640 medium (supplemented with 10% FBS, 1% penicillin-streptomycin, and 2 mM L-glutamine) (Merck, UK).

4.2. DC Generation and Culture

CD14+ monocytes were isolated from PBMCs using magnetic bead-based positive selection (Miltenyi Biotec, Bergisch Gladbach, Germany) according to the manufacturer's protocol. Isolated monocytes were resuspended at 1 × 10^6 cells/mL in RPMI 1640 medium supplemented with 10% FBS, 1% penicillin-streptomycin, and 2 mM L-glutamine, and plated in 48-well flat-bottom tissue culture-treated plates (Corning, Corning, NY, USA). For differentiation into immature DCs (iDCs), 50 ng/mL recombinant human GM-CSF and 20 ng/mL recombinant human IL-4 (both from R&D Systems, Minneapolis, MN, USA) were added. Cultures were maintained at 37°C in a humidified 5% CO_2 incubator for 5 days, with 50% media and cytokine replenishment on day 3. On day 5, non-adherent and loosely adherent cells were gently harvested, and the medium was replaced with serum-free X-VIVO 15 (Lonza, Walkersville, MD, USA). iDCs were then stimulated with 100 ng/mL LPS (from Escherichia coli O111:B4; Sigma-Aldrich, St. Louis, MO, USA) and/or 10 µg/mL ovalbumin (OVA; Grade V, Sigma-Aldrich) for 24 h to induce maturation into mature DCs (mDCs). Maturation status was confirmed by flow cytometric analysis of surface markers (e.g., CD80, CD83, CD86, HLA-DR). The cells were from cell culture and centrifuged with 1 mL of phosphate buffer albumin (PBA) at 300g for 5 minutes, the supernatant was kept for use in EV isolation, the pellet was re-suspending by gentle tapping. Antibodies were then added to the FACS tubes per manufacturer instructions and incubated at 4°C for 30 min. After the incubation, 2 mL of PBA was added and washed at 300g for 5 min. Supernatants were discarded and 300 µl of fixation buffer was added. The samples were analysed on SONY ID7000 flow cytometer.

4.3. Naïve T Cell Isolation

Naive CD4+ T cells were isolated from matched donor whole blood via negative magnetic selection using the Naive CD4+ T Cell Isolation Kit II (Miltenyi Biotec, Bergisch Gladbach, Germany), following the manufacturer's instructions. PBMCs were first isolated as described above. Isolated PBMCs were resuspended in MACS buffer (PBS containing 2 mM EDTA and 0.5% BSA) at 1 × 10^7 cells/mL. Naive CD4+ Biotin-Antibody Cocktail II (10 µL per 10^7 cells) was added, and the mixture was incubated at 4°C for 5 min. Subsequently, MACS buffer (30 µL per 10^7 cells) and Naive CD4+ MicroBeads II (20 µL per 10^7 cells) were added, followed by incubation at 4°C for 10 min. Labelled cells were loaded onto a pre-equilibrated LS MACS column in the magnetic field (Miltenyi Biotec). Unlabelled naive CD4+ T cells in the flow-through were collected, while the column was washed thrice with 3 mL MACS buffer. The eluted fraction was centrifuged at 300 × g for 5 min at 4°C, and the cell pellet was resuspended in serum-free AIM-V medium (Thermo Fisher Scientific, Waltham, MA, USA) at 1 × 10^6 cells/mL. Naive T cells (2 × 10^5 cells in 200 µL) were aliquoted into 96-well U-bottom tissue culture plates (Corning) for downstream assays. Purity was verified by flow cytometry (>95% CD3+CD4+CD45RA+CCR7+). Extracellular markers were stained by the previously described method.

4.4. EV Isolation with Size-Exclusion Chromatography

Following 24 h stimulation with LPS and OVA, DC culture supernatants were harvested and centrifuged at 300 × g for 8 min at 4°C to remove cellular debris. Clarified supernatants were subjected to size-exclusion chromatography (SEC) using qEVoriginal/35 nm columns (IZON Science, Oxford, UK) equilibrated with sterile-filtered PBS (0.22 µm pore size). Columns were pre-washed with 2 mL PBS, excess buffer was removed, and 1 mL supernatant was loaded per column. As the sample entered the resin bed, an additional 1 mL PBS was added to initiate elusion. Nine EV-enriched fractions (corresponding to elution volumes 1.5-4.5 mL) were collected based on manufacturer

 doi:10.20944/preprints202512.1321.v1

guidelines. Fractions were pooled and concentrated using Amicon Ultra-0.5 10 kDa centrifugal filter units (Merck Millipore, Burlington, MA, USA). Pooled eluates (up to 500 µL) were loaded into filters and centrifuged at 4000 × g for 10 min at 4°C. Retentates containing concentrated EVs were recovered from the upper chamber, resuspended in 100-200 µL PBS. The EVs were used immediately for the 1st dose of EVs, and for subsequent use was stored in -20°C for 24 h until next dose.

4.5. Nano-Tracking Analysis

Nano-tracking analysis (NTA) was performed on solutions containing EVs in order to confirm their sizes and presence. NTA was considered as the gold standard for sizing EVs. The ZetaView (Particle Matrix) was used for NTA. EVs isolated via SEC were diluted 1:1000 in 0.22 µM filtered PBS and loaded into an LM10/14 Nanosight instrument (Nanosight, Malvern Panalytical, UK) for particle size distribution and quantification. Before analysis, the instrument's sensitivity was calibrated using a 1:10 dilution of 100 nm carboxylated polystyrene nanoparticles (IZON) and a 1:1000 dilution of 200 nm polystyrene nanoparticles (Malvern Panalytical). Automatic settings were used for minimum expected particle size, minimum track length, and blur. The instrument was configured with a sensitivity of 78, a gain of 26.88, and a temperature of 21 °C. National Institute of Standards and Technology (NIST) beads were analysed at a sensitivity of 65. Data processing and particle size distribution analysis were conducted using NTA Software 3.3 Dev build 3.3.301 (Malvern Panalytical).

4.6. Enzyme-Linked Immunosorbent Assay

After SEC had been performed, each of the fractions (1 to 7) were collected and used in ELISA to evaluate the effectiveness of SEC clearing capabilities of cytokines from EV solutions. 96-well plates were coated with IL-6 and IL-8 capture antibodies by adding 100µl of coating solution in each well, ensuring that the solution covers the bottom of each well evenly. The plate was then incubated overnight at 4 °C to allow the capture antibodies to adsorb on the bottom of the wells. After incubation the coating solution was discarded, and the wells were washed with PBS+0.05%Tween20. To prevent non-specific binding of proteins to the plate, the plates were blocked with blocking buffer for 1h. After the blocking of the plate, the blocking buffer was removed, and the wells were washed with PBS+0.05%Tween20. The sample was then added to the wells and incubated for 2h at room temperature, to allow the cytokines to bind to the capture antibodies. The wells were then washed with PBS+0.05%Tween20 to remove unbound substances and minimize the background noise. Horseradish peroxidase (HRP) Streptavidin was added to the wells and incubated for 1h at room temperature. The wells were washed again. 3,3',5,5' tetramethylbenzidine (TMB) was added to the wells to initiate a reaction with HRP and allowed to incubate for 20 min in the dark at room temperature. The stop solution (Sulfuric acid) was added to cease the reactions between HRP and TMB. The plate was then inserted into a microplate reader to measure the absorbance at 450nm and 570nm. The results from the standards were then plotted in a standard curve. Utilizing the standard curve, it was possible to calculate the concentrations of IL-6 and IL-8 in the solution.

4.7. DC-T Cell Assay

Isolated DC-derived EVs were added to naive CD4+ T cell cultures (2 × 10^5 cells/well in 200 µL AIM-V medium), with EV replenishment every 24 h for up to 3 days. For co-stimulation assays, 96-well U-bottom plates were pre-coated for 1h at 4°C with 2 µg/mL anti-human CD3 (clone OKT3; BioLegend, San Diego, CA, USA) in PBS, washed twice with PBS. Anti-human CD28 (2 µg/mL; clone CD28.2; BioLegend) was added directly to wells. Cultures were incubated at 37°C in a humidified 5% CO_2 incubator for 72 h total. After 30h of stimulation, protein transport inhibitor cocktail (GolgiPlug; BD Biosciences, Franklin Lakes, NJ, USA; 1 µL/mL) was added, and cells were incubated for an additional 12 h. Harvested cells were washed once with PBA (PBS containing 0.1% BSA and 0.09% sodium azide) by centrifugation at 300 × g for 10 min at 4°C. For extracellular staining, cells were

 doi:10.20944/preprints202512.1321.v1

resuspended in 100 µL PBA containing fluorochrome-conjugated antibodies against CD3, CD4, CD45RA, CD27, CD28, CCR7, and CD69 (all from BioLegend) and incubated at 4°C for 30 min in the dark. Cells were washed twice with PBA (300 × g, 5 min), fixed in 500 µL fixation buffer (BD Biosciences) for 30 min at 4°C. For intracellular staining, fixed cells were washed with 2 mL 1× Perm/Wash buffer (BD Biosciences; 500 × g, 5 min) and resuspended in 100 µL Perm/Wash buffer containing antibodies against IL-2, IL-4, IFN-γ, and TNF-α (all from BioLegend). Samples were incubated at room temperature for 30 min in the dark, washed twice with PBA (500 × g, 5 min), and resuspended in 300 µL fresh fixation buffer for storage at 4°C until acquisition. Stained samples were acquired on a Sony ID7000 spectral flow cytometer (Sony Biotechnology, Tokyo, Japan) using 405 nm, 488 nm, 561 nm, and 638 nm lasers, collecting data for 2 min per sample at a flow rate of ~1000 events/s. Spectral unmixing and compensation were performed with Sony software (v2.0.4), followed by manual gating in Kaluza and FlowJo software.

4.8. Supervised Flow Cytometry Analysis

Acquired spectral flow cytometry data were analysed using Kaluza Analysis software (v2.1; Beckman Coulter, Brea, CA, USA). A manual hierarchical gating strategy was applied: initial selection of viable singlets (forward/side scatter area vs. height, followed by live/dead amine-reactive dye exclusion), then CD3+CD4+ lymphocytes, and further subsetting to naive T cells (CD45RA+CCR7+). Expression of activation (CD69), costimulatory (CD27, CD28), and chemokine receptor (CCR7) markers, along with intracellular cytokines (IL-2, IL-4, IFN-γ, TNF-α), was quantified as percentage positive within the naive CD4+ gate. Gating was performed on fluorescence-minus-one controls for compensation and isotype controls for positivity thresholds. Aggregated data were imported into GraphPad Prism (v10.1.1; GraphPad Software, San Diego, CA, USA) for visualization. Statistical significance was assessed using two-way ANOVA with Sidak's post-hoc correction for donor group comparisons (healthy vs. allergic; $\alpha = 0.05$), and one-way ANOVA with Brown-Forsythe correction for condition effects within groups (unstimulated vs. EV-stimulated; $\alpha = 0.05$). Differences were deemed significant at $p < 0.05$.

4.9. Unsupervised Flow Cytometry Analysis

Flow cytometry data were additionally processed in FlowJo v10.8.1 (BD Biosciences, Franklin Lakes, NJ, USA) for unsupervised clustering. Following import, samples underwent manual hierarchical gating to select viable CD3+CD4+ naive T cells (CD45RA+CCR7+). The 'Downsample' plugin was applied to standardize each sample to 10,000 events, minimizing batch effects. Samples were concatenated by experimental condition (e.g., donor group or EV stimulation type) to generate combined files. Optimal cluster number was estimated using the 'Phenograph' plugin. This value was input into the FlowSOM plugin to delineate self-organizing map clusters. Resultant clusters were visualized via tSNE. 'Cluster Explorer' was employed to generate annotated t-SNE plots (color-coded by marker expression or population frequency) and quantify event distributions per cluster.

4.10. Statistical Analysis

Statistical analyses were performed using GraphPad Prism version 10.1.1 (GraphPad Software, San Diego, CA, USA). Data are presented as individual data points with median and interquartile range or as mean ± SEM where indicated. Normality was assessed using the Shapiro–Wilk test. For comparisons between healthy and allergic donor groups across multiple conditions, two-way repeated-measures ANOVA was used, followed by Šídák's multiple comparisons test. Differences between stimulation conditions within the same donor group were evaluated by one-way repeated-measures ANOVA with Brown–Forsythe correction or Friedman test, followed by Dunn's multiple comparisons test where appropriate. Differences were considered statistically significant at $p < 0.05$. For statistical comparisons of the unsupervised clustering analysis, the percentage of naive T cells per cluster was calculated for each donor. Data were exported to GraphPad Prism and analysed using

 doi:10.20944/preprints202512.1321.v1

multiple Mann-Whitney U tests (unpaired, two-tailed) with false discovery rate (FDR) correction at 5% via the two-stage step-up (Benjamini, Krieger, and Yekutieli) method for healthy vs. allergic donor differences. Condition-specific effects within allergic donors were evaluated by multiple Wilcoxon matched-pairs signed-rank tests with the same FDR correction ($\alpha = 0.05$).

The overall assay workflow is illustrated in Figure 7.

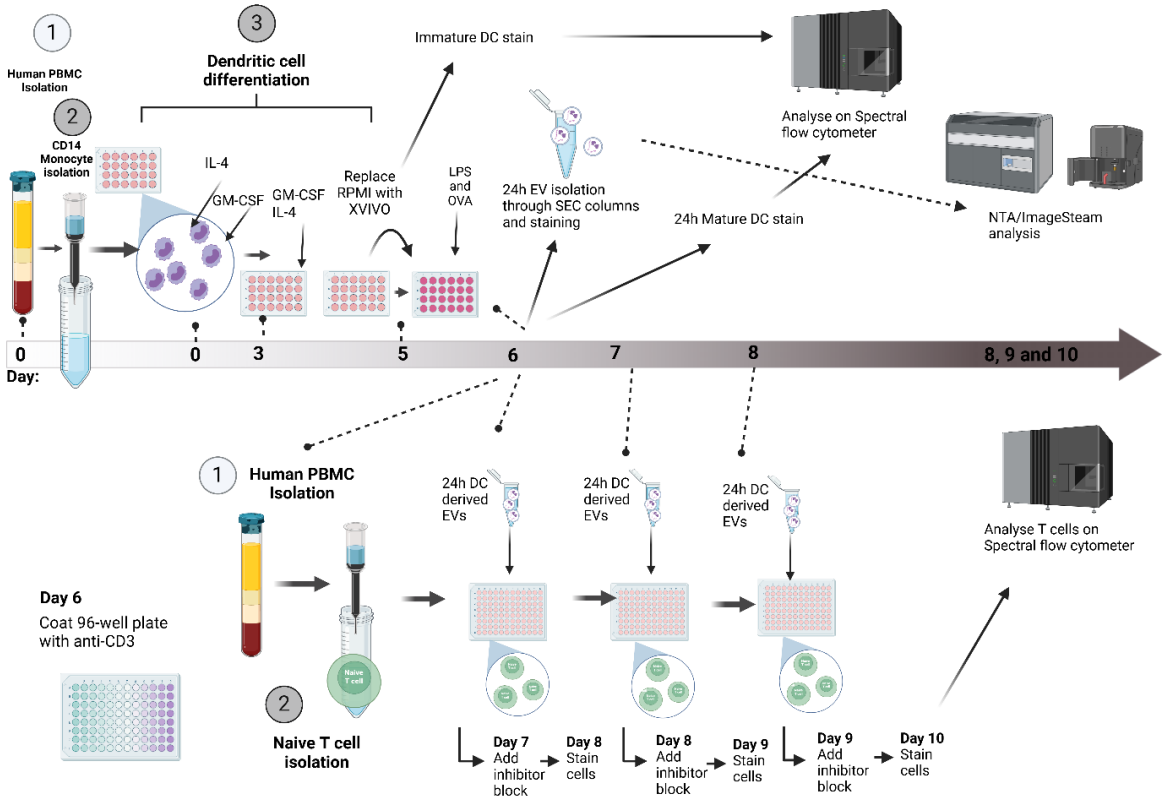

Figure 7. DC-EV and T cell assay setup. On day 0, human whole blood was collected, and PBMCs were isolated by density gradient (1), followed by CD14+ monocyte isolation using magnetic separation (2). Monocytes were cultured in 48-well tissue culture plates with GM-CSF and IL-4 stimulation in RPMI + 10% FBS to initiate differentiation in dendritic cells, on day 3 the media and cytokines were replenished. On day 5 the media was swapped to serum-free media X-VIVO and stimulated with LPS, OVA and OVA+LPS (3). On day 6 EVs from DCs were collected and isolate through SEC, alongside PBMC 2nd isolation and negative selection of naïve T cells using magnetic separation (1,2). Naïve T cells were exposed to DC EVs for 3 separate doses, and the cells were collected and stained for extracellular and intracellular markers.

Supplementary Materials: The following supporting information can be downloaded at the website of this paper posted on Preprints.org.

Author Contributions: D.T. undertook the data generation, refined the methodology and wrote the manuscript. G.H. aided in data generation and helped write the manuscript. L.C.F., V.J., and D.O. planned the experiment design and reviewed the manuscript. All authors have read and agreed to the published version of the manuscript.

Funding: The ID7000C spectral cell analyser was funded by the Biotechnology and Biological Sciences Research Council (BBSRC) to L.F. and D.O. (Grant Ref BB/T017619/1). The ImageStream X MKII was funded by the Welcome to L.F. and D.O. (Grant Ref 212908/Z/18/Z).

Institutional Review Board Statement: This study was approved by the NHS Health Research Authority Research Ethics Committee (Ref 21/SC/0183.

Informed Consent Statement: Informed consent was obtained from all subjects involved in the study.

 doi:10.20944/preprints202512.1321.v1

Data Availability Statement: The original contributions presented in the study are included in the article; further inquiries can be directed to the corresponding author.

Acknowledgments: We thank the volunteers who provided blood samples for the study, as well as the research nurses at Cripps Health Centre, Nottingham for obtaining subject blood samples. We also thank the flow cytometry facility at the University of Nottingham for providing flow cytometry advice.

Conflicts of Interest: The authors declare no conflicts of interest.

Abbreviations

The following abbreviations are used in this manuscript:

BSA	Bovine serum albumin
CD	Cluster of Differentiation
DC	Dendritic Cells
EDTA	Ethylenediaminetetraacetic acid
EV	Extracellular Vesicle
FBS	Fetal bovine serum
IFN	Interferon
IgE	Immunoglobulin E
IL	Interleukin
LPS	Lipopolysaccharide
MHC	Major Histocompatibility Complex
MISEV	Minimal Information for Studies of Extracellular Vesicles
OVA	Ovalbumin
PBS	Phosphate-buffered saline
SEC	Size-exclusion chromatography
t-SNE	t-distributed stochastic neighbour embedding
Th2	T helper 2 cells
TNF	Tumour necrosis factor

References

1. Sicherer, S.H. and H.A. Sampson, Food allergy: A review and update on epidemiology, pathogenesis, diagnosis, prevention, and management. J Allergy Clin Immunol, 2018. 141(1)**: P**. 41-58.
2. Loh, W. and M.L.K. Tang, The Epidemiology of Food Allergy in the Global Context. Int J Environ Res Public Health, 2018. 15(9).
3. Leech, S.C.**; et al.**, BSACI 2021 guideline for the management of egg allergy. Clinical & Experimental Allergy, 2021. 51(10)**: P**. 1262-1278.
4. Lambrecht, B.N. and H. Hammad, The immunology of the allergy epidemic and the hygiene hypothesis. Nat Immunol, 2017. 18(10)**: P**. 1076-1083.
5. Gowthaman, U.**; et al.**, Identification of a T follicular helper cell subset that drives anaphylactic IgE. Science, 2019. 365(6456).
6. Curtsinger, J.M. and M.F. Mescher, Inflammatory cytokines as a third signal for T cell activation. Curr Opin Immunol, 2010. 22(3)**: P**. 333-40.
7. Welsh, J.A.**; et al.**, Minimal information for studies of extracellular vesicles (MISEV2023): From basic to advanced approaches. J Extracell Vesicles, 2024. 13(2)**: P**. e12404.
8. Robbins, P.D. and A.E. Morelli, Regulation of immune responses by extracellular vesicles. Nat Rev Immunol, 2014. 14(3)**: P**. 195-208.
9. Tkach, M. and C. Théry, Communication by Extracellular Vesicles: Where We Are and Where We Need to Go. Cell, 2016. 164(6)**: P**. 1226-1232.
10. Lindenbergh, M.F.S. and W. Stoorvogel, Antigen Presentation by Extracellular Vesicles from Professional Antigen-Presenting Cells. Annu Rev Immunol, 2018. 36**: P**. 435-459.

 doi:10.20944/preprints202512.1321.v1

11. Colombo, M.**; et al.**, Analysis of ESCRT functions in exosome biogenesis, composition and secretion highlights the heterogeneity of extracellular vesicles. J Cell Sci, 2013. 126(Pt 24)**: P**. 5553-65.
12. Vallhov, H.**; et al.**, Exosomes containing glycoprotein 350 released by EBV-transformed B cells selectively target B cells through CD21 and block EBV infection in vitro. J Immunol, 2011. 186(1)**: P**. 73-82.
13. Vallhov, H.**; et al.**, Dendritic cell-derived exosomes carry the major cat allergen Fel d 1 and induce an allergic immune response. Allergy, 2015. 70(12)**: P**. 1651-5.
14. Théry, C., M. Ostrowski, and E. Segura, Membrane vesicles as conveyors of immune responses. Nat Rev Immunol, 2009. 9(8)**: P**. 581-93.
15. Simonsen, J.B., What Are We Looking At? Extracellular Vesicles, Lipoproteins, or Both? Circ Res, 2017. 121(8)**: P**. 920-922.
16. Takov, K., D.M. Yellon, and S.M. Davidson, Comparison of small extracellular vesicles isolated from plasma by ultracentrifugation or size-exclusion chromatography**: Yield**, purity and functional potential. J Extracell Vesicles, 2019. 8(1)**: P**. 1560809.
17. Kornilov, R.**; et al.**, Efficient ultrafiltration-based protocol to deplete extracellular vesicles from fetal bovine serum. J Extracell Vesicles, 2018. 7(1)**: P**. 1422674.
18. Chen, T.**; et al.**, Extracellular vesicles as vital players in drug delivery**: A** focus on clinical disease treatment. Front Bioeng Biotechnol, 2025. 13**: P**. 1600227.
19. Guan, S.**; et al.**, Characterization of Urinary Exosomes Purified with Size Exclusion Chromatography and Ultracentrifugation. J Proteome Res, 2020. 19(6)**: P**. 2217-2225.
20. Nordin, J.Z.**; et al.**, Ultrafiltration with size-exclusion liquid chromatography for high yield isolation of extracellular vesicles preserving intact biophysical and functional properties. Nanomedicine, 2015. 11(4)**: P**. 879-83.
21. Fang, S.B.**; et al.**, Plasma EVs Display Antigen-Presenting Characteristics in Patients With Allergic Rhinitis and Promote Differentiation of Th2 Cells. Front Immunol, 2021. 12**: P**. 710372.
22. Molfetta, R.**; et al.**, Immune complexes exposed on mast cell-derived nanovesicles amplify allergic inflammation. Allergy, 2020. 75(5)**: P**. 1260-1263.
23. Dehnavi, S.**; et al.**, Loading Ovalbumin into Mesenchymal Stem Cell-Derived Exosomes as a Nanoscale Carrier with Immunomodulatory Potential for Allergen-Specific Immunotherapy. Reports of Biochemistry and Molecular Biology, 2023. 11(4)**: P**. 626-634.
24. Asadirad, A.**; et al.**, Sublingual prophylactic administration of OVA-loaded MSC-derived exosomes to prevent allergic sensitization. Int Immunopharmacol, 2023. 120**: P**. 110405.
25. Liu, W.**; et al.**, Development of allergic rhinitis immunotherapy using antigen-loaded small extracellular vesicles. Journal of Controlled Release, 2022. 345**: P**. 433-442.
26. Kang, C.**; et al.**, Role of dendritic cell-derived exosomes in allergic rhinitis (Review). Int J Mol Med, 2023. 52(6).